Polymer 51 (2010) 4160–4168

Contents lists available at ScienceDirect

Polymer

journal homepage: www.elsevier.com/locate/polymer

Characteristic phase behavior of polybutadiene-*block*- poly(ε-caploractone)/polybutadiene blend after melting crystalline-amorphous alternating lamellar structure

Hideaki Takagi [a], Katsuhiro Yamamoto [a,*], Shigeru Okamoto [a], Shinichi Sakurai [b]

[a] Graduate School of Engineering, Department of Materials Science & Technology, Nagoya Institute of Technology, Gokiso-cho, Showa-ku, Nagoya 466-8555, Japan
[b] Department of Polymer Science & Engineering, Kyoto Institute of Technology, Matsugasaki, Sakyo-ku, Kyoto 606-8585, Japan

ARTICLE INFO

Article history:
Received 19 January 2010
Received in revised form
22 June 2010
Accepted 25 June 2010
Available online 17 July 2010

Keywords:
Semi-crystalline block copolymer
Melting process
Equilibrium structure

ABSTRACT

The phase behavior after melting of crystalline-amorphous alternating lamella structure (CA-LAM) and cooling from disordered state in polybutadiene-*block*-poly(ε-caprolactone) (PB-*b*-PCL)/PB homopolymer blends was investigated using small-angle X-ray scattering (SAXS). As soon as CA-LAM disappeared by melting, coexistence of hexagonally packed cylinder (HEX) and layer structure was confirmed. On further increasing temperature, HEX transited to Gyroid (Gyr) and the layer structure still remained (the layer gradually disappeared or transited to HEX and Gyr at given temperatures). Under cooling process from disordered state, perforated layer (PL) structure first appeared and transformed into Gyr. Although the hysteresis of temperature dependence of domain spacing between heating and cooling process was observed, it was not observed any more when the sample was heated after aging for adequately long time. This hysteresis behavior was attributed to local distribution of PB homopolymer blended in block copolymer. When PCL chains crystallized, PB homopolymer was expelled out of PB domain. With the temperature increased and aging for a time, the PB homopolymer was redistributed into the PB domain and the equilibrium structures in this system were observed.

1. Introduction

Block copolymers are well known to form periodic morphologies with long-range order. It is well known that those equilibrium morphologies are spheres arranged in a body-centered cubic (BCC) lattice, hexagonally packed cylinder (HEX), gyroid structure (Gyr), *Fddd* structure [1], and lamellar structure (LAM). The morphology formed in molten state is predicted by χN and f (χ is the Flory–Huggins interaction parameter, N is the total degree of polymerization and f is the volume fraction of one block).

In the past decade, order–order phase transition (OOT) has attracted much attention both theoretically [2–5] and experimentally [6–16]. It has been reported that hexagonally perforated layers (HPL) appear as non-equilibrium structure between OOT [8–20]. The stacking sequence of HPL channels can be modeled as ABCABC… (face-centered cubic lattice type) [14–17] and ABAB… (hexagonally closed packed lattice type) pattern [16–18]. In addition, it was reported that there is a transient PL phase with irregularly perforated channels [19,20].

The crystallization behavior of crystalline-amorphous block copolymer is extensively studied [21–33]. When crystalline-amorphous block copolymer is crystallized, it shows complex phase behavior compared with amorphous–amorphous block copolymer. When glass transition temperature (T_g) is higher than crystallization temperature (T_c), or segregation power is relatively strong, the morphology forming in molten state is maintained after crystallization [21–29]. In contrast, when T_g is lower than T_c, and segregation power is relatively weak, the morphology forming in molten state transforms to crystalline-amorphous alternating lamellar (CA-LAM) structure during crystallization [28–32]. The crystallization behavior and kinetics of crystalline-amorphous block copolymer/amorphous homopolymer blends are also studied [24–28,31,32]. Recently, in polybutadiene-*block*-poly(ε-caploractone) (PB-*b*-PCL)/polybutadiene homopolymer blends, it was reported that a fraction of PB homopolymer was expelled out of the PB lamellar domain during PCL crystallization [32].

To our knowledge, the process of phase transition from CA-LAM to morphology forming in molten state has not been extensively studied [31,33]. Nojima et al. investigated a melting behavior of CA-

* Corresponding author. Tel./fax: +81 52 735 5277.
E-mail address: yamamoto.katsuhiro@nitech.ac.jp (K. Yamamoto).

0032-3861/$ – see front matter © 2010 Elsevier Ltd. All rights reserved.
doi:10.1016/j.polymer.2010.06.047

LAM, and they indicated that there was a correlation hole in phase transition from CA-LAM to BCC [31]. Recently, Weiyu et al. reported that crystalline lamellae composed of polyehyrene-*block*-poly (etherene oxide) (PE-*b*-PEO) formed Gyr phase after melting of PEO block, and then Gyr phase transformed into HEX phase with PE block crystallized. Finally, after melting of PE block, HEX phase transformed into spherical morphology [33].

As mentioned above, in PB-*b*-PCL/PB blends, since PB homopolymer does not dispersed uniformly into PB domain in CA-LAM, characteristic phase behavior was anticipated when PB homopolymer was redistributed into PB domain after melting of CA-LAM. In this paper, we reported characteristic phase behavior of PB-*b*-PCL/PB blends after melting of CA-LAM.

2. Experimental section

2.1. Materials

Polybutadiene-block-poly(ε-caploractone) (PB-*b*-PCL) semicrystalline diblock copolymers were synthesized by anionic polymerization under vacuum. The butadiene monomer in toluene was first polymerized at 50 °C for 3 h using *n*-butyllithium as the initiator. After completing the polymerization of the butadiene monomer, a small amount of polybutadiene/toluene solution is poured in a glass tube attached with the reaction container under vacuum. The glass tube was sealed off and the content was obtained to evaluate molecular weight of the precursor polybutadiene block. And then ε-caploractone monomer was added through another glass tube connected with the reaction container in order to synthesize the block copolymer at 4 °C. The polybutadiene homopolymer which was used for blending with the PB-*b*-PCL was synthesized by anionic polymerization under vacuum. All samples were characterized by size exclusion chromatography (SEC) and ^{1}H nuclear magnetic resonance spectroscopy (^{1}H NMR). Melting point (T_m) is defined as the temperature at which the temperature dependent SAXS invariant drastically changed in melting process. Neat sample of the synthesized PB-*b*-PCL form a lamellar structure (LAM) in molten state, and crystalline-amorphous alternating lamellar structure (CA-LAM) in crystalline state. Table 1 shows the molecular characteristics of the diblock copolymers and homopolymer used in this study. Blend samples were prepared as follows: after dissolving a predetermined amount of PB-*b*-PCL and PB homopolymer into toluene with a total polymer concentration of ca. 5 wt%, the solvent was slowly evaporated. After complete removal of the solvent, the cast sample was dried in vacuum for a long time (at least 48 h) at room temperature. Blend samples are denoted as bBCL*x* where *x* means the apparent volume fraction of PCL block. All blend samples were confirmed to form CA-LAM in crystalline state.

2.2. Synchrotron radiation small-angle X-ray scattering

The SAXS measurements with synchrotron radiation were conducted at the beamline 15A in Photon Factory (PF) of High Energy Accelerator Research Organization in Tukuba, Japan (KEK), and BL40B2 in SPring-8 of Japan Synchrotron Radiation Research Institute, Hyogo, Japan. In BL-15A, a charge-coupled device (C7300) with an image intensifier (Hamamatsu Photonics Co., Ltd.) (II-CCD) was used as a detector, and detector was set at a position of 230 cm apart from sample position. The wavelength λ of X-rays was 0.150 nm. In BL40B2, the imaging plate (Rigaku R-axis IV) was used as a detector, and detector was set at a position of 300 cm apart from sample position. The wavelength λ of X-rays was 0.150 nm. The sample temperature was controlled using Linkam LK-600 M (Japan Hightech). Collagen was used as a standard specimen to calibrate SAXS detector. The scattering intensities were corrected for background scattering and sample absorption. All one-dimensional SAXS profiles were obtained by circularly averaging two-dimensional SAXS patterns. The magnitude of scattering vector (q) is given by

$$q = \frac{4\pi}{\lambda}\sin\left(\frac{\theta}{2}\right) \tag{1}$$

where λ is the wavelength of the X-ray and θ is the scattering angle.

The domain spacing D is given by

$$D = \frac{2\pi}{q^*} \tag{2}$$

where q^* is the position of the first order peak.

To estimate the fraction of layer phase, double the first order peaks in SAXS profiles are decomposed by using Lorenz peak function. From the evaluated peak areas A_{layer} and A_{HEX}, the fraction of layer phase was defined by

$$\phi_{\mathrm{layer}} = \frac{A_{\mathrm{layer}}}{A_{\mathrm{HEX}} + A_{\mathrm{layer}}} \tag{3}$$

2.3. Laboratory-scale small-angle X-ray scattering

Laboratory-scale SAXS measurements were conducted using a Nano-Viewer (Rigaku Corporation) equipped with a rotating anode X-ray generator operated at 40 kV and 20 mA. The imaging plate (Rigaku R-axis IV) was used as a detector. The detector was set at a position of 110 cm apart from sample position. The wavelength λ of X-ray was CuKα radiation (=0.154 nm).

Table 1
Characteristics of synthesized polymers.

Code	M_n[a]	M_w/M_n[a]	f_{PCL} (vol%)[b]	T_m (°C)[c]	Crystalline state[c]	Molten state[c]
PB-*b*-PCL	7600	1.06	57	55	CA-LAM	lamellar
PB	700	–	–	–	–	–

[a] Determined by size exclusion chromatography (SEC).
[b] Determined by ^{1}H NMR.
[c] Determined by SAXS.

3. Results and discussion

3.1. Phase behavior in heating process

Fig. 1(a) shows SAXS profiles for bBCL39 at a heating rate of 5 °C/min. Fig. 1(b) shows the enlarged SAXS profiles in the vicinity of the first order peak in Fig. 1(a). At 25 °C, where the sample was fully crystallized, the diffraction peaks are seen at a relative q-peak position of 1:2. This indicates that the sample formed a crystalline-amorphous alternative lamellar structure (CA-LAM) in the crystalline state. In the temperature range from 70 to 130 °C above melting point of PCL, an additional scattering peak near the high q side of the first order peak was observed. The first order peak seems to be asymmetric and have a shoulder at high q side and double peaks clearly observed at 110 °C. The diffraction peaks are observed at relative q-peak position of 1:1.06:1.75:2.03:2.18:2.71:3.29. Details of this structure with these q-peak positions are discussed next section. When the temperature reached at 140 °C, the observed SAXS profile was different from that below 130 °C. The relative diffraction peak positions at 140 °C were 1:1.04:1.15:1.64:1.92. In the case of gyroid structure (Gyr), peaks are generally seen at relative positions of 1:1.15:1.53:1.63:1.91. The

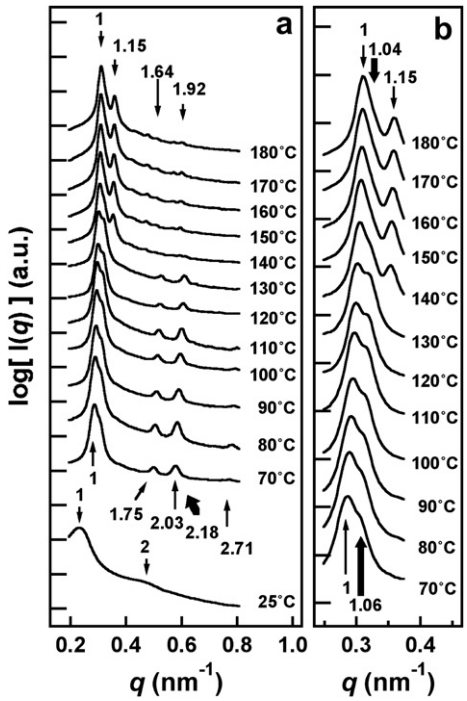

Fig. 1. (a) SAXS profiles for bBCL39 at a heating rate of 5 °C/min. (b) The enlarged SAXS profiles in the vicinity of the first order peak in Fig. 1(a). Thick arrows identify the characteristic peak position of layer structure, and thin arrows identify that of HEX (below 130 °C) and Gyr (above 140 °C).

peak positions observed above 140 °C are in good agreement with that of Gyr phase except for the peak position of 1.04. Thus, it was found that Gyr and another structure corresponding 1.04 coexisted in the observed temperature during this heating process.

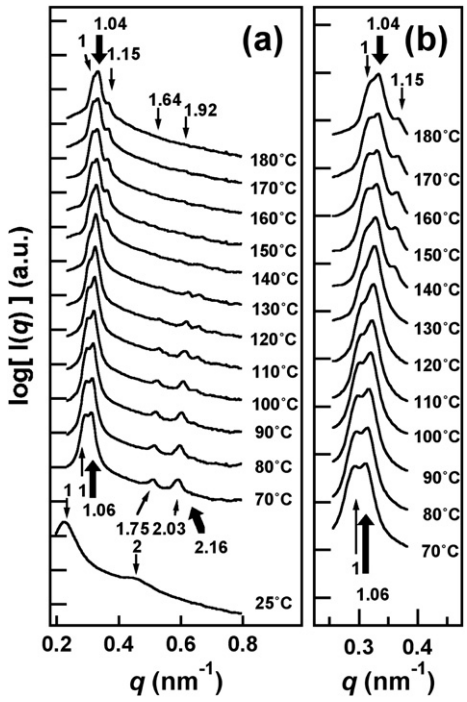

Fig. 2. (a) SAXS profiles for bBCL42 at a heating rate of 5 °C/min. (b) The enlarged SAXS profiles in the vicinity of the first order peak in Fig. 2(a). Thick arrows identify the characteristic peak position of layer structure, and thin arrows identify that of HEX (below 130 °C) and Gyr (above 140 °C).

Fig. 2(a) shows SAXS profiles for bBCL42 at a heating rate of 5 °C/min. Fig. 2(b) shows the enlarged SAXS profiles in the vicinity of the first order peak in Fig. 2(a). Similarly to the case of bBCL39, since the diffraction peaks are seen at a relative q-peak position of 1:2 in the crystalline state, the sample formed CA-LAM. The scattering peak from bBCL42 was observed near the high q side of the first order peak in the temperature range from 70 to 130 °C. From observed relative peak positions (1:1.06:1.75:2.03:2.16:3.29) for bBCL42, the structure formed in this temperature range was found to be identical with that formed in bBCL39. When temperature rose to 140 °C, the diffraction peaks were observed at relative peak position of 1:1.04:1.15:1.64:1.92, which means the Gyr structure formed above 140 °C, and another structure (corresponding 1.04q^*) coexisted with Gyr as the same as the case of bBCL39.

3.2. Determination of the morphology observed in heating process

In order to identify the structure formed in the temperature range from 70 to 130 °C in both samples bBCL39 and bBCL42, SAXS measurement of share-oriented samples of bBCL42 was conducted at SPring-8. Fig. 3(a) shows two-dimensional (2D) SAXS image

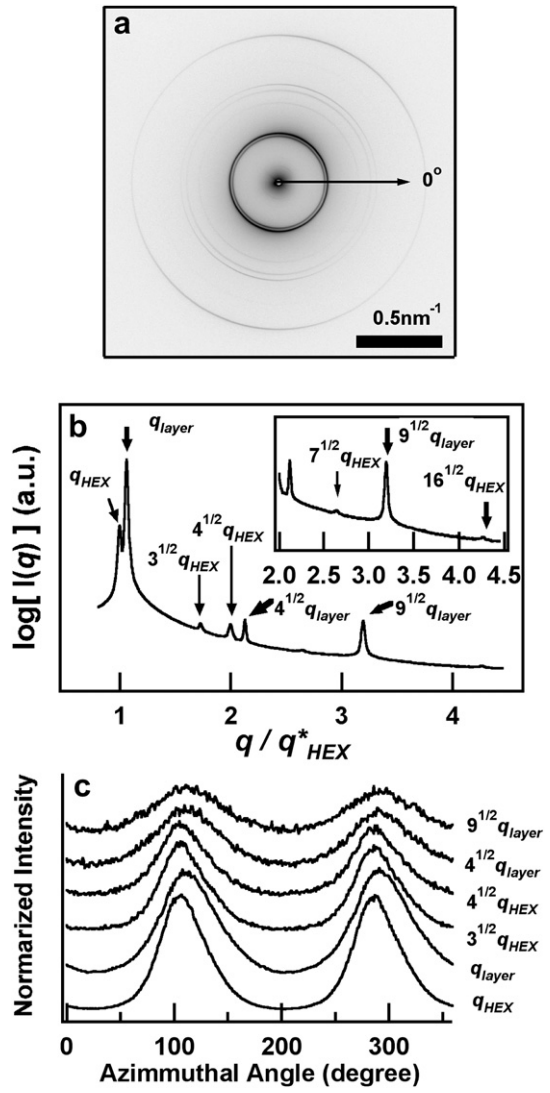

Fig. 3. (a) Two-D SAXS image of share-oriented samples of bBCL42 at 80 °C in SPring-8. (b) One-D SAXS profile obtained by circularly averaging 2D SAXS pattern in Fig. 3(a). (c) Azimuthal angle dependence of diffraction maxima for the pattern observed in Fig. 3(a).

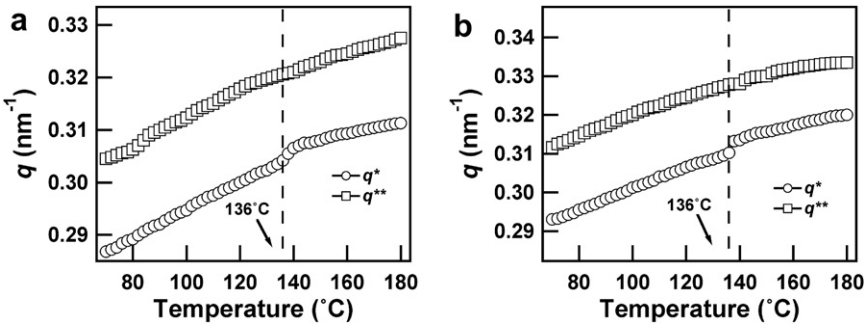

Fig. 4. The plots of the first diffraction peak q^* and second diffraction peak q^{**} versus temperature in bBCL39 (a) and in bBCL42 (b) at a heating rate of 5 °C/min.

measured at 80 °C which indicated an azimuthal angle dependent scattering ring. That is, the two arc scattering were clearly observed at around 110° and 290° with respect to the equator (clock wise rotation). One-dimensional (1D) SAXS profile accumulated by circularly averaging of 2D SAXS pattern is shown in Fig. 3(b). The scattering intensity is presented as a function of q/q^* with q^* being the position of the first diffraction peak. The same diffraction peaks with a relative q-peak position of 1:1.06:1.73:2.00:2.13:2.64:3.20:4.27 were reproduced, that is, it was identical with those in Fig. 1. If the first diffraction peak is originated from the hexagonally packed cylinder phase (HEX), the observed peak ratio of 1:1.73:2.00:2.64 is in fairly good agreement with the calculated peak ratio for HEX, except for the peaks with ratio of 1.06, 2.13, 3.20 and 4.27 which are seen in integral multiple. The rest of the peaks, thus, are assigned to the layer. It has been reported that an intermediate structure such as hexagonally perforated layer (HPL) appears in order–order transition (OOT) from/to Gyr. When HPL is measured by using SAXS, a relative q-peak position of diffraction peaks in 1D SAXS profiles are seen in multiple integer [9] and/or hexagonal [18,19] pattern. The stacking sequence of HPL channels can be modeled as ABCABC… and ABAB… pattern. In HPL structure with ABCABC… stacking, the first order and the second order peak corresponds to (100) and (002), respectively [17]. Because this two scattering plans are not parallel each other, the scattering peaks of the first order and the second order peak never be observed at the same azimuthal angle even if X-ray beam enter the sample from any directions. In HPL structure with ABAB… stacking, the first order and second order peak corresponds to (101) and (003), respectively [17]. In this case, scattering peaks of the first order and the second order peak also never be observed at the same azimuthal angle because two scattering planes are not parallel. Azimuthal angle dependent of oriented sample can reveal if the sample is HPL, or not. Fig. 3(c) shows azimuthal angle dependence of diffraction maxima for the 2D SAXS pattern except for the peak at higher q ($2.64q^*$ and $4.27q^*$) because of weaker scattering intensity. The scattering intensity was normalized with its scattering maxima. The first diffraction peak represents q_{HEX}, and the second diffraction peak represents q_{layer}. In our case, the first and the second diffraction peaks were observed at almost the same azimuthal angle. The structure corresponding to the first diffraction peak is HEX because HEX is thermodynamically stable structure as discussed later. Here, the peaks of lamellar structure (LAM) are generally seen at integral multiple. As mentioned above, the diffraction peaks of HPL can be seen in the same manner. In addition, PL phase with irregularly perforated channels also gives peaks in integral multiple, and diffused scattering shoulder is seen at the low q side of the first order peak. Therefore, it is difficult to identify the structure corresponding to the second diffraction peak by only SAXS measurement. Since it was still unclear whether the layer is perforated or not, we simply use the term of "layer" in this paper. Therefore, it was concluded that the structure formed in bBCL39 and bBCL42 at 80 °C was coexistence of HEX and layer.

Above 140 °C, the structure with $1.04q^*$ cannot be clearly identified because any higher order peaks were absent in SAXS profiles in Figs. 1 and 2. Fig. 4(a and b) show plots of q^* and q^{**} versus temperature for bBCL39 and bBCL42, respectively, at a heating rate of 5 °C/min. The slope of q^* discontinuously changed around 136 °C. This indicates that OOT from HEX to Gyr occurred around at this temperature. On the other hand, the slope of q^{**} nearly continuously changed. Therefore, the layer structure observed below 136 °C did not undergo OOT on heating, and accordingly coexistence of Gyr and layer structure was confirmed above 136 °C.

3.3. Thermodynamical stability of coexisting state

Although coexistence of HEX and layer was observed after melting, whether, or not, is the coexisting of those thermodynamically stable? The isothermal SAXS measurement in the temperature range where the HEX and layer coexisted was conducted. The sample of bBCL39 was heated from room temperature

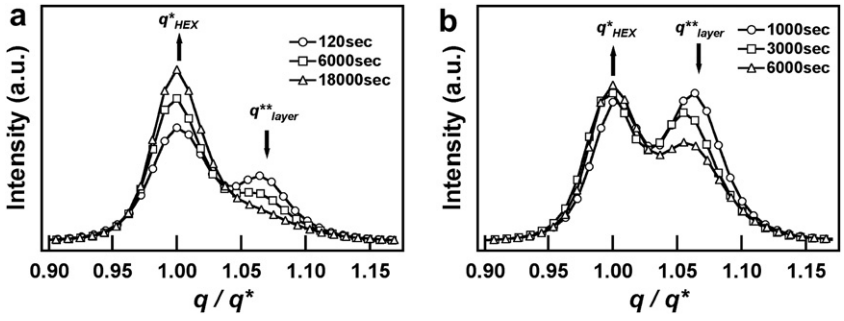

Fig. 5. (a) Time-dependent SAXS profiles of bBCL39 at (a) 80 °C and (b) 120 °C.

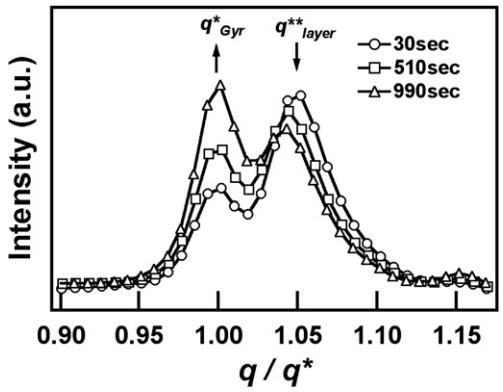

Fig. 6. Time-dependent SAXS profiles of bBCL42 at 180 °C. The sample was heated from room temperature (crystalline state) to 80 °C at a heating rate of 100 °C/min, and held for 30 min at 80 °C. And then sample was re-heated from 80 °C to 180 °C at a heating rate of 10 °C/min.

(crystalline state) to 80 or 120 °C (above melting point) at a heating rate of 100 °C/min, and then the scattering date was accumulated just after temperature reached at 80 or 120 °C. The isothermal time-dependent SAXS profiles at 80 and 120 °C were shown in Fig. 5 (a and b), respectively. The scattering profile is presented as a function of q/q^* with q^*_{HEX} being the position of the first diffraction peak of HEX. The first order peak of layer is represented by q^{**}_{layer}. The scattering intensity of the HEX increased and the scattering intensity of the layer decreased with passing time. This indicates that the layer is relatively unstable structure in the coexisting region of HEX and layer.

At higher temperature range than where Gyr structure appeared ($T > 136$ °C), the Gyr and the layer also coexisted as mentioned above. The isothermal SAXS measurement was conducted in order to check the stability of the layer in the coexisting region. The time-dependent SAXS profiles of bBCL42 at 180 °C where the Gyr and layer coexisted were shown in Fig. 6. The scattering profile is presented as a function of q/q^* with q^*_{Gyr} being the position of the first diffraction peak of Gyr. The first order peak of layer is represented

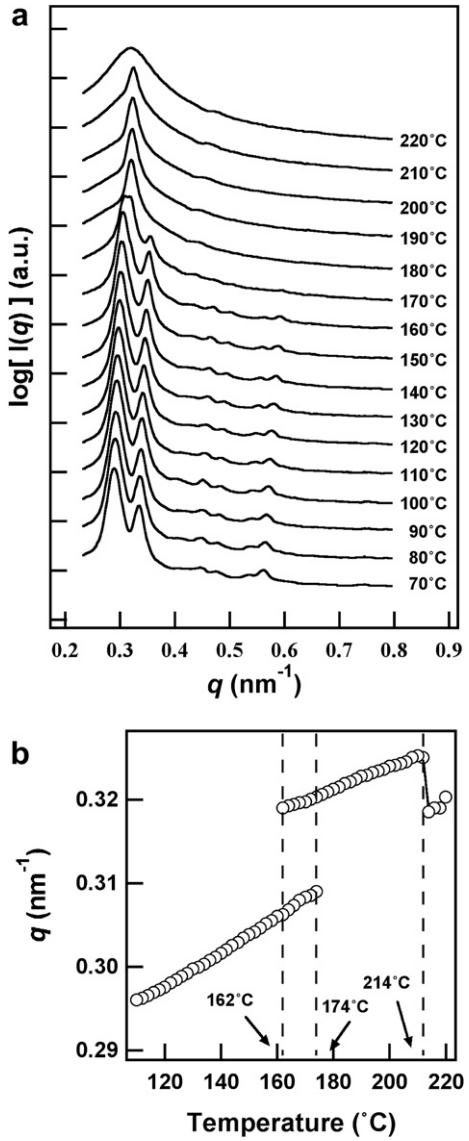

Fig. 7. (a) SAXS profiles for bBCL39 at a cooling rate of 5 °C/min. (b) The plots of peak position q^* versus temperature.

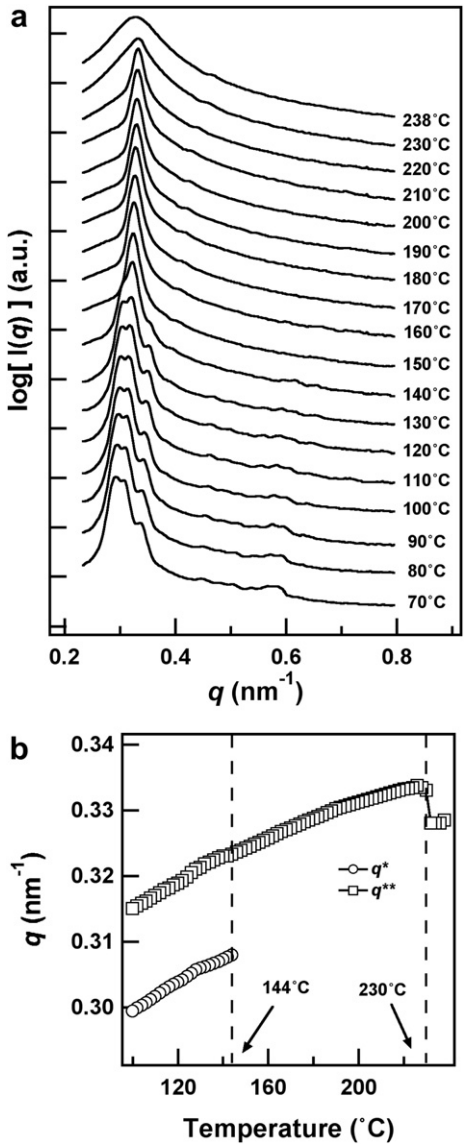

Fig. 8. (a) SAXS profiles for bBCL42 at a cooling rate of 5 °C/min. (b) The plots of peak position q^* versus temperature.

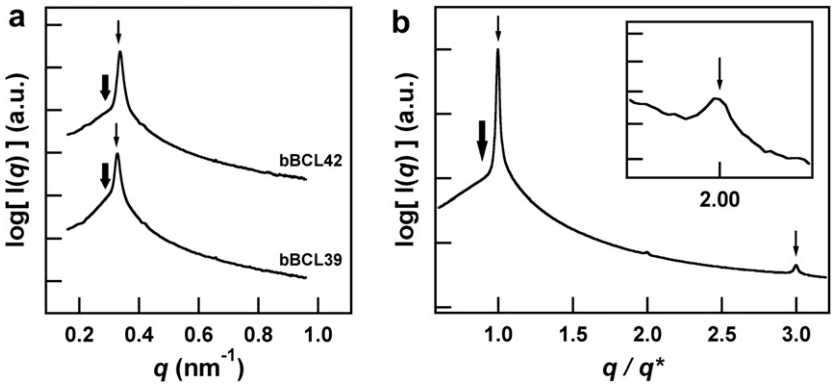

Fig. 9. (a) SAXS profile for bBCL39 and bBCL42. (b) SAXS profile for bBCL42 obtained at BL40B2 of SPring-8. The profiles observed at 180 °C after cooling from disordered state at a cooling rate of 100 °C/min.

by q^{**}_{layer}. The scattering intensity of Gyr increased and the scattering intensity of layer decreased with aging time. It was found that the layer was unstable in the temperature range where the Gyr and layer coexisted.

Recently, in PB-*b*-PCL/PB blends, it was reported that a fraction of PB homopolymer was expelled out of the PB lamellar domain during crystallization. Therefore, the appearance of coexisting state might be caused by this phenomenon. To identify that HEX observed just after melting of CA-LAM is not metastable phase, we investigated the phase behavior in cooling process in the next section. It is anticipated that domain spacing of HEX formed after melting of CA-LAM is small, since h-PB does not distribute uniformly in the microdomain. In the last section, we investigated temperature dependence of domain spacing between heating process and cooling process.

3.4. Phase behavior in cooling process

It is important to investigate the phase behavior in cooling process to compare with that of heating process. Then, cooling experiment from disordered state was conducted. Fig. 7(a) shows SAXS profiles for bBCL39 at a cooling rate of 5 °C/min. Fig. 7(b) shows plots of q^* against observation temperature. At 220 °C, the SAXS profile shows only one broad peak with small scattering intensity that is ascribed to the scattering from correlation hole in the disordered phase of block copolymer. As the sample was cooled to 210 °C, the sharp diffraction originating from micro-phase separation was observed. In Fig. 7(b), since the position of q^* discontinuously changed at 214 °C, the sample exhibited disorder–order transition. When the sample was cooled to 174 °C, the new scattering peak appeared (as a shoulder) in lower q side of the first order peak observed above 174 °C. The second order peak of Gyr corresponding to new scattering peak was observed at 170 °C, and the Gyr coexisted with the structure appeared above 174 °C in the temperature range from 174 to 162 °C. Upon further decrease in temperature from 162 °C, finally only Gyr was observed. The phase transition from Gyr to HEX in bBCL39 was not observed at a cooling rate of 5 °C/min. As for bBCL42, the similar phase behavior was observed except for transition temperature and time. Fig. 8(a) shows SAXS profiles for bBCL42 at a cooling rate of 5 °C/min. Fig. 8 (b) shows the temperature dependence of q^*. Discontinuous change in q^* at 230 °C (OOT from disorder to order state) was observed and at 144 °C additional new peak emerged. In the cases of bBCL42 as well as bBCL39, transformation from Gyr to HEX at a cooling rate of 5 °C/min was not observed.

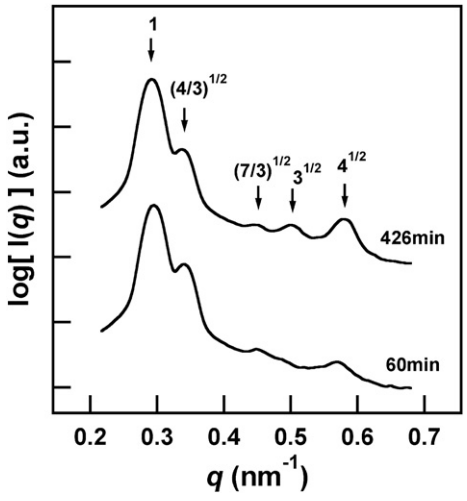

Fig. 10. SAXS profiles for bBCL35. The sample was cooled from disordered state at a cooling rate of 100 °C/min and stored at 80 °C.

In order to identify the structure observed after quenching from disordered to the ordered state, SAXS profiles of both bBCL39 and bBCL42 obtained at 200 °C after cooling from disordered state is shown in Fig. 9(a) which observed in BL-15A at PF. SAXS profiles show only one sharp scattering peak (marked by thin arrow) and the diffuse scattering (marked by thick arrow). Since any other higher order peaks were not observed in Fig. 9(a) (These may be buried in noise of the detector), the structure cannot be identified with only these measurements. SAXS measurement in the beamline of BL40B2 at SPring-8 was conducted to reveal whether higher order peaks exist. The SAXS profile for bBCL42 was obtained at SPring-8 after quenching to 180 °C at a cooling rate of 100 °C/min as shown in Fig. 9(b). The inset indicates enlarged profile around q/q^* of 2.0. Diffraction peaks were clearly observed at a relative q-peak position of 1:2:3 (marked by thin arrows), and the diffuse scattering peak was observed at the low q side of the first order peak (marked by thick arrow). This structure was reported as a transient PL phase with irregularly perforated channels [19,20]. Therefore, it was concluded that transient PL appeared before forming Gyr in cooling process. Although SAXS measurement was not conducted for bBCL39 at SPring-8, since diffuse scattering peak was observed at the low q side of the first order peak as shown Fig. 9(a), PL structure formed during transition to Gyr as well as bBCL42.

In cooling process, the phase transition from Gyr to HEX was not observed in both bBCL39 and bBCL42 at a cooling rate of 5 °C/min. Additionally, when the Gyr samples obtained at 180 °C were cooled to 80 °C in both samples, transformation from Gyr into HEX did not

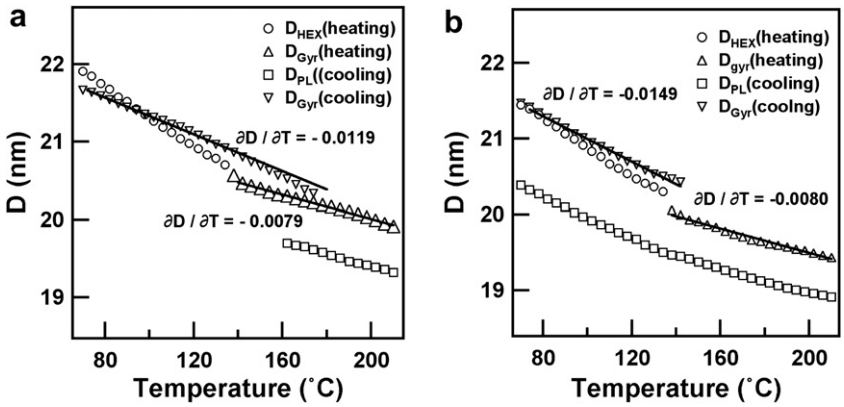

Fig. 11. Change in domain spacing D for bBCL39 (a) and bBCL42 (b) in heating and cooling process, respectively. Structures for bBCL39 were HEX below 136°C and Gyr above 136°C during heating process, and PL above 162°C and Gyr below 162°C during cooling process. Those for bBCL42 were HEX below 136°C and Gyr above 136°C in heating process, and Gyr below 144°C.

occur even after aging for 6 h (Figure is not shown). Here, we used the blend sample of bBCL35 to confirm the phase transition Gyr to HEX in cooling process. It was confirmed that bBCL35 showed coexisting of HEX/layer at lower temperature and revealed that of Gyr/layer at higher temperature as well as bBCL39 and bBCL42 in heating process (Figure is not shown). As for bBCL35, cooling experiment from disordered state to 80 °C at a cooling rate of 100 °C/min indicated different result. SAXS profiles for bBCL35 are shown in Fig. 10 which was detected by the Nano-Viewer. In Fig. 10, the second order peak of Gyr corresponding to relative q-position of $(4/3)^{1/2}$ was clearly seen after 60 min, and the peak at a relative q-position of $4^{1/2}$ was also seen with somewhat weak intensity. After annealing for 426 min, the scattering intensity of $(4/3)^{1/2}$ corresponding to Gyr decreased, and peaks at $3^{1/2}$ and $4^{1/2}$ corresponding to HEX developed. Thus, in the case of bBCL35, transition from Gyr to HEX was observed. The blend sample of bBCL35 can easily relax the polymer chain to transform into HEX phase in comparison with the samples of bBCL39 and bBCL42, because the amount of PB homopolymer added in bBCL35 was larger than that in bBCL39 and bBCL42 as a result PB homopolymer acted as a plasticizer. Thus, we believe that the aging time was too short to induce the phase transition from Gyr to HEX in the both cases of bBCL39 and bBCL42, which is related to the PCL volume fraction. The sample of bBCL35 was most asymmetric among samples used here. Thus, HEX formed in bBCL35 is most thermodynamically stable than other samples, because the PCL composition is close to HEX boundary in phase diagram. Namely, the effect of both composition and plasticizer is considered to drive the phase transition from Gyr to HEX was observed in bBCL35.

Let us consider the order of the phase. The systems transform from Gyr → HEX during cooling. The general phase diagram [34] of amorphous block copolymers is the transition from HEX → Gyr → LAM (lamellar microdomain in amorphous block copolymer) at a fixed composition with decreasing temperature. In a blending system, the analogy with the phase diagram of block copolymer in selective solvent [35] must be taken into account. Blend of homopolymer PB in PB-*b*-PCL corresponds to decreasing the apparent volume fraction of PCL and thus a "horizontal" trajectory in a phase diagram. In this case, PB-*b*-PCL itself shows the lamellar morphology in molten state. After blending, bBCL shows cylindrical one. With increasing temperature, χN of the bBCL system decreases ("vertical" trajectory in a phase diagram) and the selectivity of PB must be weak. The loss of the selectivity brings the reduction of the apparent volume fraction of PCL. These considerations can explain the morphology travels from "HEX to Gyr and subsequently to LAM with decreasing temperature. Therefore, it is reasonably possible that the phase order HEX → Gyr – (Gyr → HEX in cooling) is observed as in the system of block copolymers in a selective solvent. However, the strangeness for PB-*b*-PCL itself remains in non-blend system (without blending). As we previously reported the phase behavior of PB-*b*-PCL, the phase transitions from HEX to Gry in heating process and from Gyr to HEX in cooling process were observed at the volume fraction of PCL around 35% [36]. Namely, the phenomenon of the phase orders mentioned here

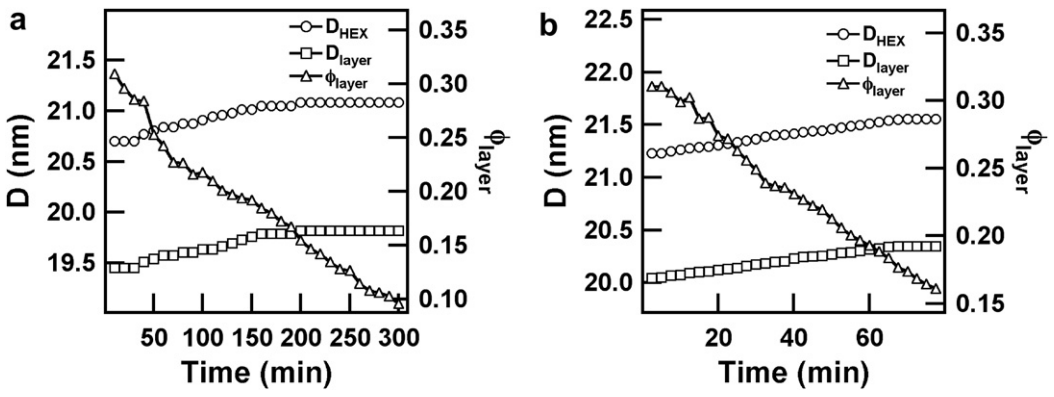

Fig. 12. The time evolution of D_{HEX}, D_{layer}, and ϕ_{layer} calculated using eq(3) for bBCL39 at (a) 80 °C and (b) 120 °C.

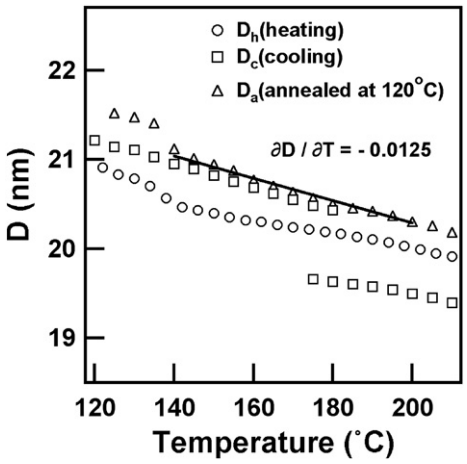

Fig. 13. Change in domain spacing D for bBCL39. Triangles (D_a) represent HEX below 136 °C and Gyr above 136 °C during heating process after aging at 120 °C for. Data with circles (D_h) and squares (D_c) are identical with those in Fig. 11(a).

is not unique to the blend or selective solvent systems. It can be safely said that it is specific behavior for PB-*b*-PCL whose molecular weight is relatively small and which can be oligomer rather than polymer.

3.5. The hysteresis behavior of D observed between heating and cooling process

Fig. 11(a) shows the change in D with temperature for bBCL39. Observed D are represented with circles for HEX below 136 °C and triangles for Gyr above 136 °C during heating process, squares for PL above 162 °C and inverted triangles for Gyr below 162 °C during cooling process. Fig. 11(b) shows plots of D against temperature in bBCL42. Solid lines in Fig. 11(a) and (b) correspond to the slope of D in the temperature range where Gyr structure formed. In Fig. 11(a), the slope of D (Gyr phase) observed above 136 °C during heating process is −0.0079 nm/°C and that of D (Gyr phase) below 162 °C during cooling process is −0.0119 nm/°C. In Fig. 11(b), the slope of D (Gyr phase) observed above 136 °C during heating process is −0.0080 nm/°C and that of D (Gyr phase) below 144 °C during cooling process is −0.0149 nm/°C. The slope of D was slightly different between heating and cooling process for both samples. In the higher temperature range (above 200 °C), the slopes of D during heating process in bBCL39 and bBCL42 were nearly coincident with those in cooling process. However, the value of D above 162 °C (Gyr phase) during cooling process was higher than that of D above 136 °C (Gyr phase) during heating process. Why was a large hysteresis of temperature dependence of D between heating process and cooling process observed? Recently, it was reported that a fraction of PB homopolymer (h-PB) was expelled out of the PB lamellar domain during PCL crystallization in PB-*b*-PCL/PB blends [32]. Namely, the macro-phase separation between PB-*b*-PCL and h-PB occurred during crystallization, and then h-PB rich domain (h-PB domain) localized between CA-LAM. In our cases, the same situation can be considered when PB-*b*-PCL/PB blend was crystallized. The composition of local area around block copolymer can be expected to be lower h-PB fraction. The HEX observed after melting CA-LAM may also have inadequate domain spacing, because h-PB was not uniformly distributed in the PB domain of HEX. Similarly, Gyr phase transited from HEX with inadequate domain spacing was still also the same situation during heating process. On the other hand, once sample heated up to the disordered state, h-PB was fully mixed with PB-*b*-PCL. In the ordered phase observed during cooling process from the disordered state, since h-PB fully dispersed in PB domain, Gyr structure has equilibrium and adequate domain spacing. As indicated in Fig. 11(a) and (b), the both D during heating process approached the D extrapolated to high temperatures in cooling process, which means the expelled h-PB gradually dispersed into the PB domain and the structure reached equilibrium. It can be easily anticipated that the excluded h-PB can dispersed into the PB domain when the sample is aged for long time, and also expected that no hysteresis of D between heating and cooling process is observed when the h-PB fully is dissolved into the PB domain of HEX in heating process. Then, the isothermal SAXS measurements at 80 and 120 °C where HEX and layer coexisted were conducted during melting process. The time evolution of D_{HEX}, D_{layer}, and apparent fraction of ϕ_{layer} estimated from the time-dependent SAXS profiles for bBCL39 at 80 and 120 °C is shown in Fig. 12(a and b), respectively. The sample was heated from room temperature (crystalline state) to 80 and 120 °C (above melting temperature) at a heating rate of 100 °C/min, and then the scattering data were accumulated just after reached at 80 and 120 °C. Circles and squares represent D_{HEX} and D_{layer}, respectively. Triangles represents ϕ_{layer} defined using eq. (3). At 80 °C (Fig. 12(a)), the values of D_{HEX} and D_{layer} increased with passing time and reached plateau (21.1 and 19.8 nm, respectively) after 200 min from temperature jump. At 120 °C (Fig. 12(b)), D_{HEX} and D_{layer} also rose with time and finally came at plateau values (21.5 and 20.3 nm, respectively) after 80 min. In contrast, the ϕ_{layer} monotonically decrease with aging time. These results indicate that the expelled h-PB distributed into the PB domain. Moreover, D_{HEX} as well as D_{layer} increased with passing time. These results indicate that the layer phase was also lack of the h-PB, and the h-PB redistributed simultaneously into both HEX and layer phase by further annealing. Fig. 13 shows the temperature dependence of D (triangles) for bBCL39 obtained on subsequently heating after the isothermal measurement of Fig. 12(b). Structures were HEX below 136 °C and Gyr above 136 °C. Data with circles (D_h) and squares (D_c) are identical with those in Fig. 11(a) to confirm an annealing effect on the temperature dependent D. The value of D_a was higher than that of D_h, and in good agreement with D_c at temperature ranging from 145 to 180 °C where Gyr phase forms. In addition, since the slope of D_a observed above 136 °C was −0.0125 nm/°C, the slope of D_h was almost coincident with that of cooling process (see Fig. 11(a)). Therefore, in the sample which was annealed for 80 min, the hysteresis of temperature dependence of D between cooling and heating process disappeared, because Gyr observed in heating process was formed from HEX where h-PB fully mixed.

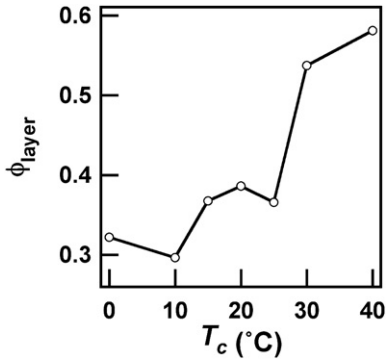

Fig. 14. The plots of ϕ_{layer} for bBCL39 versus crystallization temperature.

Now let us discuss the origin of the appearance of unstable layer phase. To reveal the effect of crystallization condition on ϕ_{layer}, the fraction ϕ_{layer} obtained from the sample of bBCL39 crystallized at various temperatures is plotted against crystallization temperature

(T_c) in Fig. 14. The sample was fully crystallized at a certain temperature T_c followed by heating to 80 °C at a heating rate of 100 °C/min, temperature was kept for 60 s. After that, SAXS date was acquired at 80 °C. It can be seen from Fig. 14 that ϕ_{layer} increases with an increase in T_c. This may result from exclusion of h-PB from domain during crystallization. In the case of high T_c, h-PB, which can be free to move in h-PB domain, is expelled out of PB domain during crystallization because of slow crystallization rate. As a result, since a large amount of h-PB is missed out of PB domain, the fraction of h-PB dissolved in PB domain of CA-LAM decreases. In other words, macro-phase separation between PB-*b*-PCL and h-PB occurs. In this situation, just after melting of CA-LAM, since HEX is formed in the vicinity of h-PB domain, and unstable layer phase formed in the region far away from h-PB domain, the coexisting of HEX and layer is observed. By further heating or annealing, h-PB in h-PB domain diffuses into PB domain. By contraries, in the low T_c, much h-PB can be arrested in PB domain because of fast crystallization rate. Since the amount of h-PB existed in PB domain of CA-LAM was relatively large, HEX easily formed just after melting of CA-LAM. Recently, however, it was reported that there exist intermediate structures during the phase transition from CA-LAM to BCC or Gyr [37,38]. It is possible that unstable layer phase appears as intermediate structure during phase transition from CA-LAM to HEX. Namely, layer phase appears as a transitional state before forming HEX, because layer structure is similar to CA-LAM (Both are layers). Therefore, it is a challenge to show clearly how unstable layer phase formed. Further investigation is needed to explain the origin of the appearance of unstable layer phase.

In this report, we could not give the direct evidence that h-PB was expelled out of the PB lamellar domain in crystallized state. However, as discussed in Figs. 11 and 12, the hysteresis of D between heating and cooling process was observed without aging in molten state. D_{HEX} obtained after melting of PCL increased by aging for long time. This result indicates that the expelled h-PB domain was redistributed into the PB domain. As discussed in Fig. 13, no hysteresis of D between heating and cooling process was observed when h-PB was remixed into the PB domain. Besides, in the phase transition from CA-LAM to Gyr or BCC by using PB-*b*-PCL (non-blended sample), neither the change of D in the isothermal measurement after melting of CA-LAM nor the hysteresis of D between heating and cooling process was observed [34]. Therefore, these results are considered as the indirect evidence that h-PB was expelled out of PB domain by crystallization.

4. Conclusions

The phase behavior after melting of CA-LAM and cooling from disordered state in PB-*b*-PCL/PB blends was investigated using SAXS. As soon as CA-LAM disappeared by melting, coexisting of HEX and layer structure was observed. Upon further increase of temperature, these blends exhibited OOT from HEX to Gyr, and then coexisting of Gyr and layer was observed. In the cooling process, transient PL structure with irregular perforated channels was observed and subsequent decrease of temperature induced transition of transient PL into Gyr. During heating process, when these blends were aged in temperature range where HEX and layer coexisted, the fraction of layer ϕ_{layer} decreased with increasing temperature. In addition, when the sample stored at 80 °C (temperature jump from R.T.) in which HEX and layer coexisted, D_{HEX} and D_{layer} increased and ϕ_{layer} also decreased with aging time. These results indicate that layer observed in the coexisting region is unstable structure, and HEX appeared after melting. CA-LAM is stable structure but does not reach completely equilibrium state. Some PB homopolymer was expelled from PB microdomain during crystallization of the sample. The temperature dependence of domain spacing corresponding to the first order peak position of Gyr observed in heating process was smaller than that of Gyr observed in cooling process. The Gyr observed in heating process was still non-equilibrium in this system just after transition from HEX because PB homopolymer was not fully distributed PB microdomain. This hysteresis behavior was caused by redistribution of PB homopolymer.

Acknowledgment

The SAXS measurement was performed under approval of the Photon Factory Program Advisory Committee (Proposal No. 2005G245 and 2006G342) and SPring-8 Program Advisory Committee (Proposal No. 2006A1060). This research was partially supported by Ministry of Education, Science, Sports, and Culture, Grant-in-Aid for Young Scientists (B) (20750176, 2008)

References

[1] Kim MI, Wakada T, Akasaka S, Nishitsuji S, Saijo K, Hasegawa H, et al. Macromolecules 2008;41:7667–70.
[2] Goveas JL, Milner ST. Macromolecules 1997;30:2605–12.
[3] Honda T, Kawakatsu T. Macromolecules 2006;39:2340–9.
[4] Matsen MW. Phys Rev Lett 1998;80:4470–3.
[5] Laradji M, Shi AC, Noolandi J, Desai RC. Macromolecules 1997;30:3242–55.
[6] Jeong U, Lee HH, Yang H, Kim JK, Okamoto S, Aida S, et al. Macromolecules 2003;36:1685–93.
[7] Kimishima K, Koga T, Hashimoto T. Macromolecules 2000;33:968–77.
[8] Mareau VH, Akasaka A, Osaka T, Hasagawa H. Macromolecules 2007;40:9032–9.
[9] Lai C, Loo YL, Register RA, Adamson DH. Macromolecules 2005;38:7098–104.
[10] Sakurai S, Umeda H, Furukawa C, Irie H, Nomura S, Lee HH, et al. J Chem Phys 1998;108:4333–9.
[11] Park H, Jung J, Chang T, Matsunaga K, Jinnai HJ. Am Chem Soc 2009;131:46–7.
[12] Hajduk DA, Takeuchi H, Hillmyer MA, Bates FS, Migild ME, Almdal K. Macromolecules 1997;30:3788–95.
[13] Wang CY, Lodge TP. Macromolecules 2002;35:6997–7006.
[14] Mortensen K, Vigild ME. Macromolecules 2009;42:1685–90.
[15] Park HW, Im K, Chung B, Ree M, Chang T, Sawa K, et al. Macromolecules 2007;40:2603–5.
[16] Zhu L, Huang P, Chen WY, Weng X, Cheng SZW, Ge Q, et al. Macromolecules 2003;36:3180–8.
[17] Ahn JH, Zin WC. Macromolecules 2000;33:641–4.
[18] Park MJ, Balsara NP. Macromolecules 2008;41:3678–87.
[19] Hamley IW, Castelletto V, Mykhaylyk OO, Yang Z, May RP, Lyakhova KS, et al. Langmuir 2004;20:10785–90.
[20] Imai M, Saeki A, Teramoto T, Kawaguchgi A, Nakayama K, Kato T, et al. Chem Phys 2001;115:10525–31.
[21] Loo YL, Register RA, Ryan AJ, Dee GT. Macromolecules 2001;34:8968–77.
[22] Zhu L, Cheng SZD, Calhoun BH, Ge Q, Quirk RP, Thomas EL, et al. Am Chem Soc 2000;122:5957–67.
[23] Loo YL, Register RA, Ryan AJ. Phys Rev Lett 2000;84:4120–3.
[24] Nojima S, Toei M, Hara S, Tanimoto S, Sasaki S. Polymer 2002;43:4087–90.
[25] Nojima S, Tanaka H, Rohadi A, Sasaki S. Polymer 1998;39:1727–34.
[26] Takeshita H, Gao YJ, Natsui T, Rodriguez TE, Miya M, Takenaka K, et al. Polymer 2007;48:7660–71.
[27] Chen HL, Hsiao SC, Lin TL, Yamauchi K, Hasegawa H, Hashimoto T. Macromolecules 2001;34:671–4.
[28] Xu JT, Fairclough JPA, Mai SM, Ryan AJ, Chaibundit C. Macromolecules 2002;35:6937–45.
[29] Loo YL, Register RA, Ryan AJ. Macromolecules 2002;35:2365–74.
[30] Shiomi T, Takeshita H, Kawaguchi H, Nagai M, Takenaka K, Miya M. Macromolecules 2002;35:8056–65.
[31] Nojima S, Kikuchi N, Rohadi A, Tanimoto S, Sasaki S. Macromolecules 1999;32:3727–34.
[32] Hsu JY, Hsieh IF, Nandan B, Chiu FC, Chen JH, Jeng US, et al. Macromolecules 2007;40:5014–22.
[33] Weiyu C, Tashiro K, Hanesaka M, Takeda S, Masunaga H, Sasaki S, et al. J Phys Chem B 2009;113:2338–46.
[34] Matsen MW. J Chem Phys 1997;106:2436–48.
[35] Hanlye KJ, Lodge TP, Huang C-I. Macromolecules 2000;33:5918–31.
[36] Takagi H, Yamamoto K, Okamoto S, Sakurai S. Koubunshi Ronbunshu 2009;66:442–9.
[37] Takagi H., Sugino Y., Hara S., Okamoto S., Yamamoto K., Shiamda S., Sakurai S. Koubunshi Ronbunshu in press.
[38] Takagi H., Hara S., Yamamoto K., Okamoto S., Sakurai S., Shimada S. Physica B. to be published.